JOC The Journal of Organic Chemistry

Note

Development of a photo-activatable Protein Phosphatase-1 Disrupting Peptide

Malgorzata Trebacz, Yansong Wang, Leslie Makotta, Lars Henschke, and Maja Köhn

J. Org. Chem., **Just Accepted Manuscript** • DOI: 10.1021/acs.joc.9b02548 • Publication Date (Web): 16 Dec 2019

JOC Note

Development of a photo-activatable Protein Phosphatase-1 Disrupting Peptide

Malgorzata Trebacz[†,‡,§,⊥], Yansong Wang[§,⊥], Leslie Makotta[§], Lars Henschke[§], Maja Köhn[†,‡,§,*]

[†]Faculty of Biology, Institute of Biology III, University of Freiburg, Schänzlestraße 18, 79104, Germany

[‡]Signalling Research Centres BIOSS and CIBSS, University of Freiburg, Freiburg, Germany.

[§]European Molecular Biology Laboratory, Genome Biology Unit, Meyerhofstraße 1, 69117 Heidelberg, Germany.

[⊥]These authors contributed equally.

*correspondence to: maja.koehn@bioss.uni-freiburg.de

ABSTRACT

We describe here the development of a photo-releasable version of a PP1-disrupting peptide (PDP-*Nal*) that triggers protein phosphatase-1 (PP1) activity. PDP-*Nal* is a 23mer that binds to PP1 through several interactions. It was photo-caged on a tyrosine residue, which required the exchange of phenylalanine in PDP-*Nal* to tyrosine in order to disrupt the most important binding interface. This PDP-*caged* can be light-controlled in live cells.

Protein phosphatase-1 (PP1) is a ubiquitously expressed phospho-serine/threonine-specific phosphatase that is involved in numerous signaling processes like cell division or insulin secretion, making it a potential therapeutic target in diseases such as cancer or diabetes.[1,2] PP1 counteracts more than 100 kinases through regulation by more than 200 regulatory interactors of protein phosphatase one (RIPPOs), with which PP1 forms holoenzymes[3,4]. The most common motif, which is involved in binding of RIPPOs, is the so-called RVxF-type motif (single amino acid abbreviation code, x = any amino acid except proline). PP1 disrupting peptides (PDPs) are currently the only selective modulators targeting the PP1 catalytic subunit, and they contain the sequence RVTF as the RVxF-type motif.[5] They disrupt a subset of PP1 holoenzymes, which results in rapid dephosphorylation of nearby substrates. PDPs were designed based on the sequence of the RIPPO nuclear inhibitor of PP1 (NIPP1)[5]. They are proteolytically stable in cellular assays[5,6] due to the incorporation of an unnatural amino acid in the sequence and because of amidation and acetylation at the *C*- and *N*-terminus, respectively[5,6]. The polybasic sequence at the *N*-terminus of PDPs was optimized to render these peptides cell-permeable[5]. Optimization of the sequence has led to the creation of PDP-*Nal* (for the sequence see Table 1), which exhibits improved stability and potency[6]. PDPs have been used to study PP1 substrates in the mitogen-activated protein kinase (MAPK) pathway[6], PP1's role in calcium release[7], and for activation of PP1 to treat arrythmia and heart failure[8,9]. Since this rather general release of PP1 activity is expected to impact several substrates and pathways, in order to study specific roles of PP1 there is a need for a more controlled modulation of its activity. Photo-cleavable groups (cages) can be used to block the interaction of a ligand to a protein. Irradiation with light releases the cage, activating the ligand that can then bind to a protein and modulate its activity. Thus, photocaging allows for temporal control by light irradiation of the ligand binding to a protein[10-12]. Nitrobenzyl derivatives are the most commonly applied photolabile protecting group. They are simple to synthesize, relatively stable, and easy to mimic with a benzyl group to screen for the optimal position of a cage in a peptide. They can be cleaved with UV light at 365 nm. Coumarin derivatives allow irradiation at longer wavelengths. Coumarins are also relatively simple to synthesize and release the substrate rapidly after visible light and two-photon irradiation. Moreover, their fluorescent properties can be used for tracking molecules inside the cells. Yet, handling them under ambient light can cause partial uncaging. Both coumarin-based and nitrobenzyl-based caging groups have been applied in cells[11-13]. Cyanine-based caging groups exhibit a similar fluorescent character and are uncaged with near-infrared light. However, the

complexity and size of the molecules can be a disadvantage[11,13]. Applications of the caging approach for peptides have been described previously. For example, nitrobenzyl-derived cages have been used to study kinase activity[14,15], have been applied in hydrogels for caging RGDS peptide in order to create a non-adhesive surface with patches containing the uncaged RGDS peptide where cells can bind[16], and for making a cell penetrating peptide light sensitive in order to enhance drug delivery to tumor cells[17]. Here, we report the development of a caged PDP for photo-control of PP1 activity. Due to the fact that most studies with caged peptides were so far done with the nitrobenzyl (Nb) cage or a derivative[14-17], and because the Nb group is relatively stable under ambient light allowing simple handling, we focused here on the Nb group as cage.

PDPs are 23mer peptides that have several interaction points with PP1[5], which could be problematic when designing a caged molecule. A single cage would only interrupt one area of interaction, and more cages might be required to efficiently disrupt the interaction between these long peptides and PP1. However, exchange of the RVTF sequence in the PDPs to RATA (this version is called "PDPm") caused the PDPs to not bind PP1 anymore[5], which provided the possibility that introducing one cage within this motif could be sufficient to disrupt the interaction PP1 with the PDP. Previously, serine was caged with a 4,5-dimethoxy-2-nitrobenzyl group (DMNb) and applied successfully in photo-release studies with peptides[14,15]. Therefore, Fmoc-Ser(DMNb)-OH was synthesized according to literature procedures[15] and incorporated into PDP-*Nal*, replacing the threonine of the RVTF sequence (PDP-*RVS(DMNb)F*). Then, the efficacy of PDP-*RVS(DMNb)F* to disrupt the PP1:Inhibitor 2 (I2) holoenzyme was tested, which would lead to free PP1 catalytic subunit that dephosphorylates an unnatural substrate (6,8-difluoro-4-methylumbelliferyl phosphate, DiFMUP) measured by a fluorescence change[5,6]. However, this modification did not significantly lower the potency of the PDP (data not shown), which was likely due to the fact that the caged serine was placed at the flexible position of the RVxF-type motif.

Due to the known importance of valine and phenylalanine of the RVTF sequence for binding of PDPs to PP1 as shown by the inactive RATA version[5], we next interrogated if caging of F and/or V would result in loss of potency. As caging of valine and phenylalanine would only be possible upon introduction of an alcohol, they were replaced by the structurally similar threonine and tyrosine. Because testing of different positions for the cage was required, for synthetic ease we used commercially available benzylated tyrosine and threonine (Table 1), mimicking the Nb group. When monitoring the potency of PDP-*Nal* and PDP-*RVTY* peptide only a slight change

was observed, with the EC_{50} changing from 144 nM to 194 nM, respectively. However, replacing valine with threonine in the PDP-*RVTY* peptide to PDP-*RTTY* led to an about 40-times higher EC_{50}, which excluded this change from further use. The benzylated PDP-*RVTY(Bn)* peptide was more than 8-times less potent that the non-benzylated PDP-*RVTY* (Table 1, Figure 1). This was judged to be a large enough difference to develop the caged PDP-*RVTY(Nb)* peptide.

Table 1. Activity of (nitro-) benzylated PDP-*Nal* derived peptides. Amino acids crucial for the binding to the pocket of PP1 carried a benzyl group (Bn) on the hydroxyl group on the side chain of the amino acid in order to mimic the Nb cage. EC_{50} values were determined by a dephosphorylation assay using recombinant PP1 and I2 with DiFMUP as substrate. The RVxF motif is marked in bold, and changes are marked in red. Error for PDP-*Nal*, PDP-*RVTY*, PDP-*RVTY(Bn)*: standard error of the mean of two independent triplicate measurements (n = 6); error for PDP-*RTTY*: standard deviation from the curve taken from one triplicate measurement (n = 3). PDP-*caged* was measured in two independent triplicate measurements, PDP-*RT(Bn)TY(Bn)* in one triplicate measurement.

Peptide	Sequence	EC_{50} [µM]
PDP-*Nal*	RRKRPKRKRKNA**RVTF***Nal*EAAEII	0.144 ± 0.040
PDP-*RVTY*	RRKRPKRKRKNA**RVTY***Nal*EAAEII	0.194 ± 0.005
PDP-*RVTY(Bn)*	RRKRPKRKRKNA**RVTY(Bn)***Nal*EAAEII	1.63 ± 0.04
PDP-*caged*	RRKRPKRKRKNA**RVTY(Nb)***Nal*EAAEII	> 1.00
PDP-*RTTY*	RRKRPKRKRKNA**RTTY***Nal*EAAEII	7.59 ± 0.89
PDP-*RT(Bn)TY(Bn)*	RRKRPKRKRKNA**RT(Bn)TY(Bn)***Nal*EAAEII	> 2.30

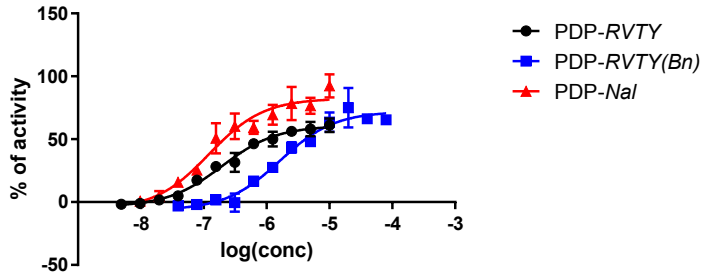

Figure 1. Difference of the kinetics of PDP-*Nal* (red triangles), PDP-*RVTY* (black dots) and PDP-*RVTY(Bn)* (blue squares). The area between the curves illustrates the activity difference between the peptides. The dephosphorylation assay was carried out with recombinant PP1 and I2 using DiFMUP as substrate. The error is the standard deviation of two independent triplicate measurements (n = 6).

First, the building block Fmoc-Tyr(Nb)-OH **1** (Scheme 1) needed to be synthesized. The synthesis of **1** had been described previously[18-20]. We adapted the synthesis procedure starting with Tyr-O*t*Bu **2** for synthetic simplicity and reported good yields[20], but optimized conditions for scaling up to several grams (Scheme 1). Firstly, the free amine was protected using Boc-anhydride. For the nitrobenzylation step, compound **3** was reacted with nitrobenzyl bromide and Cs_2CO_3 in acetonitrile (ACN), which gave compound **4** in an excellent yield of 96% at the gram scale. Deprotection of the *t*Bu-ester and the Boc-group was achieved with neat TFA, and after subsequent protection of the amine using Fmoc-OSu Fmoc-Tyr(Nb)-OH **1** was obtained in almost quantitative yield (Scheme 1). This building block was then incorporated into the PDP using standard Fmoc-solid phase synthesis, resulting in the peptide PDP-*RVTY(Nb)*, which we called PDP-*caged* (see the sequence in Table 1).

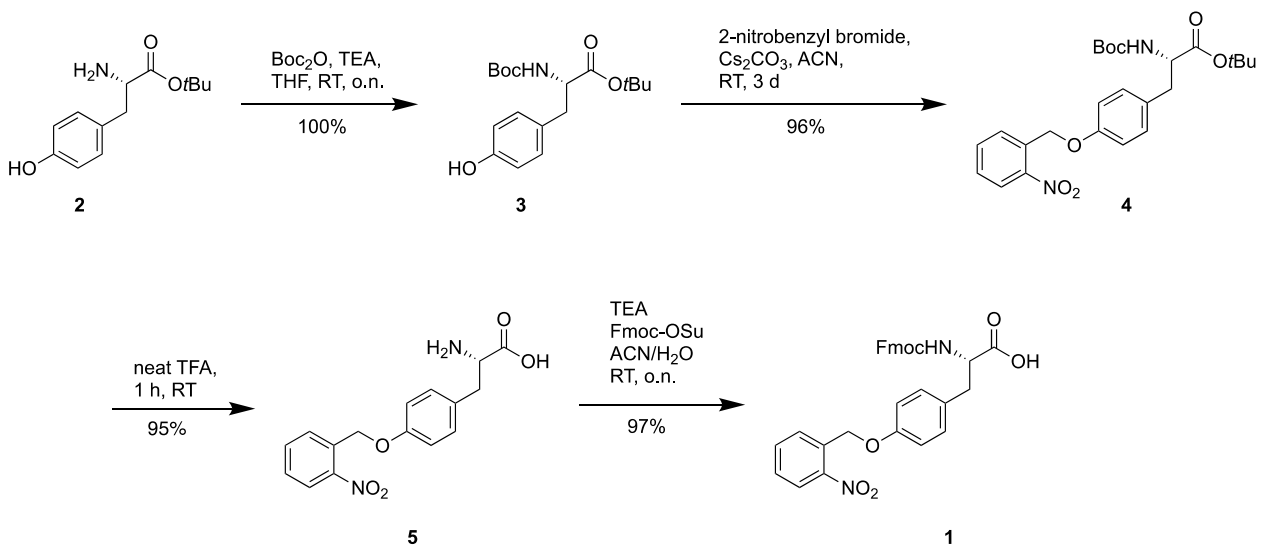

Scheme 1. Synthetis of Fmoc-Tyr(Nb)-OH **1**. ACN: acetonitrile; Boc-ON: 2-(*tert*-butoxycarbonyloxyimino)-2-phenylacetonitrile; d: day(s); DMF: *N,N*-dimethyl formamide; Fmoc-OSu: 9-fluorenylmethyl-succinimidyl carbonate; o.n.: overnight; RT: room temperature; TEA: triethylamine; *t*Bu: *tert*-buryl; TFA: trifluoroacetic acid; THF: tetrahydrofuran.

When testing PDP-*caged* in the activity assay we noted large error bars at higher concentrations and varying results (data not shown). It is possible that this was due to uncaging during the light exposure in the plate reader. Therefore, we were not able to determine an exact EC_{50}. Nevertheless, we assumed that this peptide would behave similarly to the PDP-*RVTY(Bn)*

peptide, and would disrupt the PP1:I2 interaction with a lesser potency than PDP-*RVTY*, and therefore carried on with PDP-*caged*.

Next, we characterized the stability of PDP-*caged*. After 24 hours of exposure under ambient light as well as in the dark, we did not notice any degradation (Supporting Figure S1). This confirms that the nitrobenzyl group is cleaved only with UV light, which makes it easier to handle PDP-*caged* under ambient light. We then tested if PDP-*caged* could be uncaged *in vitro*. To this end, the peptide was exposed to light at 365 nm for a certain amount of time, and the product formation to PDP-*RVTY* was monitored using HPLC. After 3 minutes the product had formed to 94%, and after 5 minutes the caged peptide was visible only in a negligible amount (Figure 2A). Finally, we asked whether a difference in activity of PDP-*caged* and PDP-*RVTY* could be detected in a cell assay, and whether the activity of PDP-*caged* could be released through uncaging. To address this, we adapted the previously established dephosphorylation of the phosphorylated threonine 3 on histone H3 (H3pT3) upon PDP treatment[5,6] to uncaging conditions. H3pT3 is a substrate of PP1 that is phosphorylated at the beginning of mitosis. The PP1:Repoman holoenzyme dephosphorylates H3pT3 at the end of mitosis, enabling mitotic exit[21,22]. PDP3 and PDP-*Nal* treatment both led to the dephosphorylation of H3pT3 during mitotic arrest[5,6]. Here, U2OS cells were synchronized in mitotic arrest and then treated with PDP-*RVTY* (positive control), PDPm-*Nal* (negative control containing the RATA sequence instead of RVTF)[6], and PDP-*caged*, or left untreated (Figure 2B). Treatment occurred with 40 μM final concentration of the peptides for 15 minutes, then the cells were washed and afterwards irradiated for 5 minutes with UV light (λ=365 nm). Following another 10 minutes of incubation, the cells were fixed and stained with antibodies against total histone H3 and H3pT3. For the experimental read-out we used the so-called *in-cell* Western method, which is similar to immunocytochemistry. The analysis showed that phosphorylation of H3pT3 was enhanced in arrested cells. As expected, treatment with PDP-*RVTY* led to a reduction of the phosphorylation level, whereas the addition of the negative control PDPm-*Nal* did not reduce the phosphorylation on H3pT3. Importantly, PDP-*caged* treatment only reduced the H3pT3 phosphorylation level after irradiation with UV light to a similar level as the positive control PDP-*RVTY* did. All other conditions were inert to UV light treatment, showing that the UV light-dependent activation is specific to PDP-*caged*. Thus, PDP-*RVTY* shows a similar activity like PDP-*Nal*[6] in this cellular assay, and the activity of PDP-*caged* can be controlled using UV light irradiation in live cells.

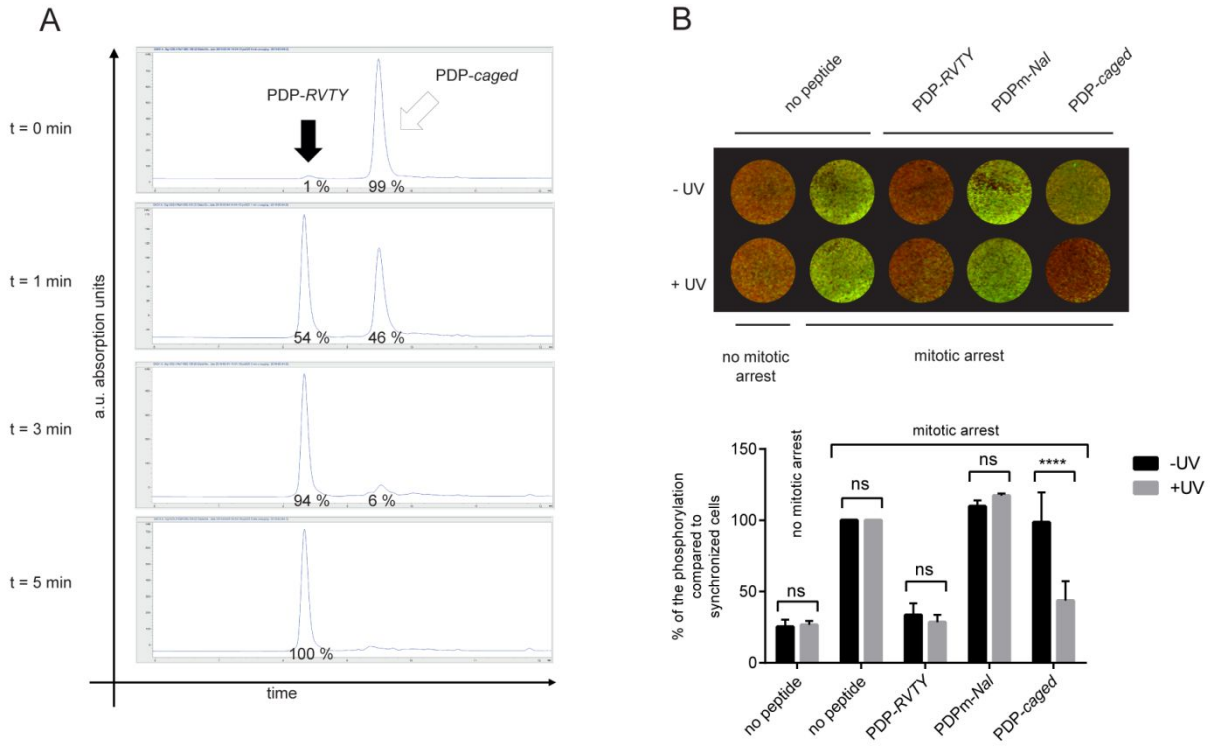

Figure 2. Uncaging experiments of PDP-*caged in vitro* and *in cells*. A) *In vitro* photo-cleavage of PDP-*caged*. HPLC traces for the peptide exposed to λ = 365 nm light for 1, 3 or 5 minutes are shown. B) Dephosphorylation of H3pT3 after treatment with 40 μM PDPs, with or without UV irradiation (+ UV/ -UV). U2OS cells were synchronized in mitotic arrest. *In-cell* Western analysis was used to detect phosphorylation levels. An inactive mutant of PDP-*Nal* containing a RATA sequence instead of RVTF was used as a negative control (PDPm-*Nal*). Red: total histone 3; green: H3pT3. The respective signal intensity of H3pT3/total histone 3 was compared to "mitotic arrest, no peptide". For quantification three independent experiments were used (see Supporting Figure S2 for the other two replicates). Results were analyzed with GraphPad Prism 6. Statistical analysis is based on 2way ANOVA and Bonferroni multiple comparison test. ($^{ns}P > 0.05$, ****$P < 0.0001$; $n = 3$).

In summary, we developed here PDP-*caged* as a light-controllable modulator of PP1 activity in live cells. While PDP-*caged* contains 23 amino acids, of which several interact with PP1[5], targeting phenylalanine of the RVxF-type binding motif for replacement with a caged tyrosine was sufficient to disrupt the interaction between the PDP and PP1. PDP-*caged* allows releasing PP1 activity in a timely precise manner through UV light irradiation at specific time points. A limitation of the Nb group when used in biological systems is that UV light irradiation is cytotoxic and has a limited penetration ability through tissue[11,12]. In the proof-of-concept settings used here, the wavelength (365 nm) is close to visible light and the irradiation time is short.

Therefore, it is not expected that the cytotoxicity would cause problems in these settings, as seen in the controls. For more complex applications however, red-shifted derivatives of Nb or Coumarin and possibly two-photon excitation might have to be applied[11,12]. We expect that this compound will prove to be a useful tool in time-sensitive studies of PP1 activity in cellular processes, such as in different stages of mitosis[23,24] and in regulation of calcium homeostasis in the heart[25].

EXPERIMENTAL SECTION

General Information. Tyr(O*t*Bu) was bought from Bachem, Switzerland. DIPEA (*N*,*N*-diisopropylethylamine), Fmoc-Thr(Bn)-OH and Fmoc-Tyr(Bn)-OH were purchased from ABCR. HOBt (*N*-hydroxybenzotriazole) was bought from MOLEKULA. Triisopropylsilane and cesium carbonate were from Alfa Aesar. Dithiothreitol (DTT), imidazole, $MnCl_2$, bovine serum albumin (BSA), pyridine, *di-tert*butyl dicarbonate (Boc_2O), triethylamine (TEA), 2-nitrobenzyl bromide, sodium hydroxide, acetic anhydride (Ac_2O) and d-chloroform were from Sigma. Dioxane, DCM (dichloromethane), Cy (cyclohexane), EA (ethyl acetate), methanol and sodium sulphate, TFA (trifluoroacetic acid), piperdine and ACN (acetonitrile) were from Roth. Other Fmoc-amino acids, 9-fluorenylmethyl-succinimidyl carbonate (Fmoc-OSu) and HBTU (*O*-(benzotriazol-1-yl)-*N,N,N',N'*-tetramethyluronium hexafluorophosphate) were from Novabiochem. Acetic anhydride and DMF (*N*,*N*-dimethylformamide) were from Merck Millipore. DiFMUP (6,8-difluoro-4-methylumbelliferyl phosphate) was purchased from Life Technologies.

^{1}H and ^{13}C Nuclear Magnetic Resonance: All spectra were recorded on a 400 MHz Bruker Avance DPX and a 500 MHz Bruker DRX. LC-MS analysis and HPLC purification: LC-MS analysis and HPLC peptide purifications were carried out on a Shimadzu High Performance Liquid Chromatograph coupled with a Mass Spectrometer using a UV-Vis Photodiode array detector SPD-M20A Prominence unless otherwise noted. ESI-MS of PDP-*caged* was performed on an Agilent Technologies 1260 Infinity I/II coupled to 6120 Quadrupole LC/MS. The solvent used for all analytical and semi-preparative runs was a mixture of H_2O containing 0.05% TFA and ACN containing 0.05% TFA. RP-HPLC analytical runs were realized with a Macherey Nagel C18 EC 250/4.0 NUCLEODUR 100-5 C18 ec column and a pump rate of 1.5 mL/min. RP-HPLC semi-preparative separations were performed with a Macherey Nagel C18 VP 250/10 NUCLEODUR 110-5 C18 ec column in gradients ranging between 31 and 43% of ACN over 30

minutes using a flow rate of 5 mL/min. Semi-preparative HPLC of PDP-*RVTY* was run on an Agilent Technologies 1260 I/II Infinity system using gradient of ACN 10 – 70% over 30 minutes. Flash chromatography: Flash chromatography purifications were performed using silica gel 60 (Roth), grain size 0.04-0.063 mm, 230-400 mesh ASTM. MALDI-TOF: The mass of all peptides was recorded on MALDI-TOF (Matrix-Assisted Laser Desorption/Ionization coupled with Time Of Flight) with the MALDI micro MX mass spectrometer (Waters, Manchester, UK) equipped with a reflection analyzer used in positive ion mode with activated delayed mode. The matrix was prepared by weighing out 10 to 20 mg of α-cyano-4-hydroxycinnamic acid (CHCA) in an Eppendorf then adding 1.0 mL of a 50:50 H_2O/ACN with 0.1% TFA final concentration.

Peptide Synthesis. All peptides were synthesized using solid phase peptide synthesis on the automated liquid handling system Syro I from Multisyntech using the Fmoc protection strategy[5,6]. Peptide elongation was carried out on the Rink Amide Resin, using HBTU/HOBT double coupling (5 eq. amino acid, 5 eq. HBTU, 2 eq. HOBt and 10 eq. DIPEA in DMF) for 40 minutes with 15 seconds vortexing every 4 minutes. The Fmoc deprotection was carried out using 20% piperidine. The capping step was done twice after every double coupling with 10 % Ac_2O/pyridine mixture for 5 minutes with 10 seconds vortexing every minute. The cleavage cocktail contained 95% TFA, 2.5% TIS and 2.5% water. After cleavage the peptides were precipitated in ice-cold diethylether, HPLC purified and analysed by MALDI (Supporting Table S1). The synthesis of PDP-*Nal* was described before[6].

Preparation of (2S)-2-tert-butyl carbamate-3-(4-hydroxyphenyl)propanoic acid *tert*-butyl ester: Boc-Tyr-O*t*Bu 3. Tyr-O*t*Bu **2** (2.00 g, 8.42 mmol), Boc_2O (1.84 g, 8.42 mmol) and TEA (114 µl, 0,84 mmol) were stirred in 100 ml THF at RT overnight. THF was removed *in vacuo*. The mixture dissolved in EA, washed three times with water, and dried over sodium sulphate. It was purified using the gradient 20%-40% EA in Cy. Yield: 2.84 g (8.42 mmol), 100%, white solid. ^{1}H NMR (400 MHz, DMSO-d6) δ 9.21 (s, 1H), δ 7.09 (d, J = 7.92 Hz, 1H), δ 7.00 (d, J = 8.36 Hz, 2H), δ 6.65 (d, J = 8.32 Hz, 2H), δ 3.91 (dt, J = 6.22, 8.38 Hz, 1H), δ 2.83 – 2.66 (m, 2H), δ 1.36 – 1.32 (m, 18H). These data are in agreement with reference [20].

Preparation of (2S)-2-tert-butyl carbamate-3-{4-[2-nitrophenyl)methoxy]phenyl} propanoic acid *tert*-butyl ester: Boc-Tyr(Nb)-O*t*Bu 4. Boc-Tyr-O*t*Bu **3** (2.76 g, 8.19 mmol), 2-nitrobenzyl bromide (1.77 g, 8.19 mmol) and Cs_2CO_3 (2.93 g, 3.00 mmol) were dissolved in ACN (30 ml). The reaction was stirred for three days at room temperature. The reaction mixture was filtered, the solvent was reduced *in vacuo*, and the compound was purified using flash chromatography

(2% EA in Cy to 10% EA in Cy). Yield: 3.70 g (7.83 mmol), 96%, orange oil. R_f = 0.45 (Cy/EA = 12/1); ^{1}H NMR ($CDCl_3$, 400 MHz) δ 8.16 (d, *J* = 8.16 Hz, 1H), δ 7.87 (d, *J* = 7.80 Hz, 1H), δ 7.66 (t, *J* = 7.56 Hz, 1H), δ 7.47 (t, *J* = 7.76 Hz, 1H), δ 7.10 (d, *J* = 8.48 Hz, 2H), δ 6.90 (d, *J* = 8.52 Hz, 2H), δ 5.45 (s, 2H) δ 5.00 (d, *J* = 8.00 Hz, 1H), δ 4.44 – 4.37 (m, 1H), δ 3.02 – 2.96 (m, 2H), δ 1.41 (s, 9H), δ 1.40 (s, 9H). ^{13}C{1H} NMR (125 MHz) δ 171.0, δ 157.0, δ 155.1, δ 146.9, δ 134.0, δ 130.7, δ 129.4, δ 128.5, δ 128.3, δ 125.0, δ 114.8, δ 82.0, δ 79.6, δ 66.8, δ 54.9, δ 37.6, δ 28.3, δ 28.0. MS *m/z*: $[M + Na]^+$ Calcd for $C_{25}H_{32}N_2O_7$ 495.21; Found $[M + Na]^+$ 495.20. These data are in agreement with reference [20].

Preparation of (2S)-2-amino-3-{4-[2-nitrophenyl)methoxy]phenyl}propanoic acid: Tyr(Nb)-OH 5. Boc-Tyr(Nb)-O*t*Bu **4** (3.70 g, 7.83 mmol) was dissolved in TFA (75 ml). The reaction was stirred for 1 h at room temperature and was monitored by thin layer chromatography (10% EA in Cy). TFA was co-evaporated with toluene *in vacuo* and the compound was dried under high vacuum. Yield: 2.35 g (7.43 mmol), 95%, orange-brown solid. The product was used further without purification and analytical data collection [20].

Preparation of (2S)-2-fluorenylmethyloxycarbamate-3-{4-[2-nitrophenyl)methoxy] phenyl}propanoic acid: Fmoc-Tyr(Nb)-OH 1. Tyr(Nb)-OH **5** (7.43 mmol), Fmoc-OSu (3.01 g, 8.92 mmol) and Et_3N (2.55 ml, 18.6 mmol) were dissolved in ACN:H_2O (7:4, 33 ml), stirred overnight at RT, dried *in vacuo* and purified using flash chromatography (DCM only, then DCM/MeOH = 12/1 and 9/1). Yield: 3.98 g (7.39 mmol), 97%, orange-brown solid. R_f = 0.47; ^{1}H NMR ($CDCl_3$, 400 MHz) δ 8.16 (d, *J* = 8.1 Hz, 1H), δ 7.86 (d, *J* = 7.8 Hz, 1H), δ 7.75 (d, *J* = 7.5 Hz, 2H), δ 7.65 (t, *J* = 7.54 Hz, 1H), δ 7.56 – 7.52 (m, 2H), δ 7.47 (t, *J* = 7.8 Hz, 1H), δ 7.39 (t, *J* = 7.4 Hz, 2H), δ 7.30 (t, *J* = 7.4 Hz, 2H), δ 7.07 (d, *J* = 8.2 Hz, 2H), δ 6.90 (d, *J* = 8.3 Hz, 2H), δ 5.43 (s, 2H), δ 5.22 (d, *J* = 7.9 Hz, 1H), δ 4.68 – 4.63 (m, 1H), δ 4.46 (dd, *J* = 10.4, 7.0 Hz, 1H), δ 4.36 (dd, *J* = 10.3, 7.2 Hz, 1H), δ 4.19 (t, *J* = 6.8 Hz, 1H), δ 3.16 (dd, *J* = 14.3, 4.9 Hz, 1H), δ 3.07 (dd, *J* = 13.9, 5.8 Hz, 1H). ^{13}C{1H} NMR (100 MHz) δ 175.5, δ 157.4, δ 155.8, δ 146.9, δ 143.7, δ 143.7, δ 141.3, δ 134.0, δ 133.8, δ 130.6, δ 128.5, δ 128.3, δ128.3, δ 127.8, δ 127.1, δ 125.0, δ 120.0, δ 115.1, δ77.2 δ 67.0, δ 66.8, δ 54.6, δ 47.2, δ 36.9. MS *m/z*: $[M + Na]^+$ Calcd for $C_{31}H_{26}N_2O_7$ 561.16, found $[M + Na]^+$ 561.15. These data are in agreement with reference [20].

Protein expression and purification. Recombinant PP1 and I2 were obtained as described in Wang et al., 2019[6].

Activity assay[6]. Recombinant PP1 protein (25 pM final assaying concentration), I2 phosphatase inhibitor (1 nM final assaying concentration), and PDP at various concentrations were incubated

in assay buffer (25 mM imidazole, 50 mM NaCl, BSA 0.1 mg/ml, 1 mM DTT, 0.3 mM $MnCl_2$, pH 7.4) for approximately 20 min at 25°C followed by addition DiFMUP to reach a final concentration of 135 μM (K_m value). The dephosphorylation of DiFMUP to the fluorescent product was monitored for 40 min on a TECAN Infinite M1000 PRO fluorescence microplate reader with excitation at 358 nm and emission at 452 nm. All experiments were performed two times in triplicates, with the exception of peptides PDP-*RTTY* and PDP-*RT(Bn)TY(Bn)*, that were measured in one triplicate. After baseline normalization (assay in the absence of PDP), the reaction rates were plotted versus the log of the inhibitor concentrations and the EC_{50} values were obtained by fitting the curves using the one-site competition model of GraphPad Prism (GraphPad Software, Version 6).

***In vitro* uncaging reaction and PDP-*caged* stability**. 100 μM PDP (10% DMSO in H_2O) was exposed to UV light using the UVP Crosslinker 365 nm (CL-1000L λ=365 nm) with the light dose 120 mJ per cm^2 or ambient light either for 3 min or for 24 hours. t = 0 control sample was kept in the dark for the time of the experiment. Samples were acquired on the Agilent HPLC system using 10-90% gradient of ACN in H_2O. Data were analysed using the OpenLAB CDS Software (Agilent).

Cell Line[6]. U2OS human female osteosarcoma cells were cultured at 37°C in a humidified incubator under an atmosphere of 5% CO_2. The cells were grown in Dulbecco's modified Eagle's medium (DMEM) containing 1 g/L glucose, 10% (v/v) fetal bovine serum (FBS), 1% (v/v) penicillin/streptomycin and 2 mM L-glutamine.

***In-cell* Western assay**[6]. *Garnier bio-one CELLSTAR* 12-well plates were coated with 0.1 mg/ml poly-D-lysine for 5 minutes, washed with PBS and led dry for 2 hours. U2OS cells were plated in 1:100 dilution one day before starting the experiment. Culture media containing 2 mM thymidine was added and after 24 h exchanged to the media without thymidine for 2 hours. Cells were treated with nocodazole for 15 h in the concentration of 100 ng/ml to allow the mitotic arrest. All peptides were diluted in the imaging buffer (115 mM NaCl, 1.2 mM $CaCl_2$, 1.2 mM $MgCl_2$, 1.2 mM K_2HPO_4, 20 mM HEPES and 2 g/l D-glucose) containing 100 ng/ml nocodazole to reach the final concentration of 40 μM and were added to the wells for 15 min. Cells were then washed with PBS and supplemented with fresh imaging buffer containing nocodazole. 5 min uncaging was conducted using the UVP Crosslinker 365 nm (CL-1000L λ=365 nm) with a light dose of 120 mJ per cm^2. Plates were placed in the incubator for another 10 min to allow PP1 activation. Cells were fixed with ice cold MeOH for 10 min, washed with PBS and blocked for 1.5 h with

Odyssey Blocking Buffer (PBS) (LI-COR). Primary antibodies against phosphorylated histone 3 on threonine 3 (H3pT3) (Millipore, cat. no. 07-424) and total histone 3 (Active Motif, cat no. 39763) in dilution 1:500 were added and incubated for 2 h. Wells were washed with In-Cell Western Washing Buffer (0.5% Triton-X in PBS) 3 times for 5 min. Secondary antibodies staining was performed using IRDye680RD Goat anti-Mouse IgG (H+L) (LI-COR, cat. no. 925-68070) and IRDye800CW Goat anti-Rabbit IgG (H+L) (LI-COR, cat. no. 925-32211) in the dilution of 1:1000 and incubated for 1 h. Wells were washed with the *in-cell* Western Washing Buffer (0.5% Triton-X in PBS) 3 times for 5 min. PBS was added and plates were acquired on the LI-COR Odyssey CLX Imager. Data analysis was carried out using the software Image Studio Lite (LI-COR).

ASSOCIATED CONTENT

Supporting Information

The Supporting Information is available free of charge on the ACS Publications website at DOI: XXX

Supporting Figure S1, S2, Supporting Table S1, NMR spectra, analytical data of compounds and peptides (pdf).

NOTES

The authors declare to have no competing financial interest.

ACKNOWLEDGEMENTS

M.K. acknowledges financial support from the European Research Council through ERC starting grant #336567 and from the German Science Foundation (DFG) through the German Excellence Strategy (BIOSS – EXC-294 and CIBSS – EXC-2189 – Project ID 390939984). Gefördert durch die Deutsche Forschungsgemeinschaft (DFG) im Rahmen der Exzellenzstrategie des Bundes und der Länder – EXC 2189 – Projekt-nummer 390939984.

REFERENCES

(1) Chatterjee, J.; Köhn, M. Targeting the untargetable: recent advances in the selective chemical modulation of protein phosphatase-1 activity. *Curr. Opin. Chem. Biol.* **2013**, *17*, 361–368.

(2) Heroes, E.; Lesage, B.; Görnemann, J.; Beullens, M.; Van Meervelt, L.; Bollen, M. The PP1 binding code: a molecular-lego strategy that governs specificity. *FEBS J.* **2013**, *280*, 584–595.

(3) Li, X.; Wilmanns, M.; Thornton, J.; Köhn, M. Elucidating human phosphatase-substrate networks. *Sci. Signal*. **2013**, *6*, rs10.

(4) Wu, D.; De Wever, V.; Derua, R.; Winkler, C.; Beullens, M.; Van Eynde, A.; Bollen, M. A substrate-trapping strategy for protein phosphatase PP1 holoenzymes using hypoactive subunit fusions. *J. Biol. Chem*. **2018**, *293*, 15152–15162.

(5) Chatterjee, J.; Beullens, M.; Sukackaite, R.; Qian, J.; Lesage, B.; Hart, D.J.; Bollen, M.; Köhn, M. Development of a peptide that selectively activates protein phosphatase-1 in living cells. *Angew. Chem. Int. Ed.* **2012**, *51*, 10054–10059.

(6) Wang, Y.; Hoermann, B.; Pavic, K.; Trebacz, M.; Rios, P.; Köhn, M. Interrogating PP1 Activity in the MAPK Pathway with Optimized PP1-Disrupting Peptides. ChemBioChem 2019, *20*, 66–71.

(7) Reither, G.; Chatterjee, J.; Beullens, M.; Bollen, M.; Schultz, C.; Köhn, M. Chemical activators of protein phosphatase-1 induce calcium release inside intact cells. *Chem. Biol*. **2013**, *20*, 1179–1186.

(8) Fischer, T.H.; Eiringhaus, J.; Dybkova, N.; Saadatmand, A.; Pabel, S.; Weber, S.; Wang, Y.; Köhn, M.; Tirilomis, T.; Ljubojevic, S.; Renner, A.; Gummert, J.; Maier, L.S.; Hasenfuß, G.; El-Armouche, A.; Sossalla, S. Activation of protein phosphatase 1 by a selective phosphatase disrupting peptide reduces sarcoplasmic reticulum Ca2+ leak in human heart failure. *Eur. J. Heart Fail.* **2018**, *20*, 1673–1685.

(9) Eiringhaus, J.; Herting, J.; Schatter, F.; Nikolaev, V.O.; Sprenger, J.; Wang, Y.; Köhn, M.; Zabel, M.; El-Armouche, A.; Hasenfuss, G.; Sossalla, S.; Fischer, T.H. Protein kinase/phosphatase balance mediates the effects of increased late sodium current on ventricular calcium cycling. *Basic Res. Cardiol*. **2019**, *114*, 13.

(10) Adams, S.R.; Tsien; R.Y. Controlling cell chemistry with caged compounds. *Annu. Rev. Physiol.* **1993***, 55,* 755–784.

(11) Brieke, C.; Rohrbach, F.; Gottschalk, A.; Mayer, G.; Heckel, A. Light-controlled tools. *Angew. Chem. Int. Ed.* **2012**, *51*, 8446–8476.

(12) Ankenbruck, N.; Courtney, T.; Naro, Y.; Deiters, A. Optochemical Control of Biological Processes in Cells and Animals. *Angew. Chem. Int. Ed.* **2018**, *57*, 2768-2798.

(13) Bardhan, A.; Deiters A. Development of photolabile protecting groups and their application to the optochemical control of cell signaling. *Current Opinion in Structural Biology* **2019,** *57*, 164–175.

(14) Dai, Z.; Dulyaninova, N. G.; Kumar, S.; Bresnick, A. R.; Lawrence, D. S. Visual Snapshot of Intracellular Kinase Activity at Onset of Mitosis. *Chem. Biol.***2007**, *14(11)*, 1254–1260.

(15) Veldhuyzen, W.F.; Nguyen, Q.; McMaster, G.; Lawrence, D.S. A light-activated probe of intracellular protein kinase activity. *J. Am. Chem. Soc.* **2003**, *125*, 13358–13359.

(16) Goubko, C. A.; Majumdar, S.; Basak, A.; Cao, X. Hydrogel cell pattering incorporating photocaged RGDS peptides **2010**, *12*, 555–568.

(17) Xie, X.; Yang, Y.; Yang, Y.; Zhang, H.; Li, Y.; Mei, X. A photo-responsive peptide- and asparagine-glycine-arginine (NGR) peptide-mediated liposomal delivery system. *Drug delivery* **2016**, *23(7)*, 2445–2456.

(18) Yamashiro, D.; Li, C.H. Adrenocorticotropins. 44. Total synthesis of the human hormone by the solid-phase method. *J. Amer. Chem. Soc*. **1973**, *95*, 1310–1315.

(19) Tatsu, Y.; Shigeri, Y.; Sogabe, S.; Yumoto, N.; Yoshikawa, S. Solid-phase synthesis of caged peptides using tyrosine modified with a photocleavable protecting group: application to the synthesis of caged neuropeptide Y. *Biochem. Biophys. Res. Commun.* **1996**, *227*, 688–693.

(20) Liu, X.; Malins, L.R.; Roche, M.; Sterjovski, J.; Duncan, R.; Garcia, M.L.; Barnes, N.C.; Anderson, D.A.; Stone, M.J.; Gorry, P.R.; Payne, R.J. Site-selective solid-phase synthesis of a CCR5 sulfopeptide library to interrogate HIV binding and entry. *ACS Chem. Biol.* **2014**, *9*, 2074–2081.

(21) Vagnarelli, P.; Ribeiro, S.; Sennels, L.; Sanchez-Pulido, L.; de Lima Alves, F.; Verheyen, T.; Kelly, D.A.; Ponting, C.P.; Rappsilber, J.; Earnshaw, W.C. Repo-Man coordinates chromosomal reorganization with nuclear envelope reassembly during mitotic exit. *Dev. Cell* **2011**, *21*, 328–342.

(22) Qian, J.; Lesage, B.; Beullens, M.; Van Eynde, A.; Bollen, M. PP1/Repo-man dephosphorylates mitotic histone H3 at T3 and regulates chromosomal aurora B targeting. *Curr. Biol*. **2011**, *21*, 766–773.

(23) Nilsson, J. Protein phosphatases in the regulation of mitosis. *J. Cell Biol.* **2019**, *218*, 395–409.

(24) Moura, M.; Conde, C. Phosphatases in Mitosis: Roles and Regulation. *Biomolecules* **2019**, *9*, pii: E55.

(25) Terentyev, D; Hamilton, S.J. Regulation of the sarcoplasmic reticulum Ca^{2+}release by serine-threonine phosphatases in the heart. *Mol. Cell. Cardiol*. **2016**, *101*, 156–164.

Table of Contents entry